1661-8726/08/01S191-16
DOI 10.1007/s00015-008-1281-1
Birkhäuser Verlag, Basel, 2008

Swiss J. Geosci. 101 (2008) Supplement 1, S191–S206

Tracing the exhumation of the Eclogite Zone (Tauern Window, Eastern Alps) by $^{40}Ar/^{39}Ar$ dating of white mica in eclogites

Walter Kurz[1], Robert Handler[2] & Christian Bertoldi[3]

Key words: $^{40}Ar/^{39}Ar$ dating, white mica, eclogite exhumation, microstructures, Subpenninic nappes, Tauern Window

ABSTRACT

New radiometric ages from the Subpenninic nappes (Eclogite Zone and Rote Wand – Modereck Nappe, Tauern Window) show that phengites formed under eclogite-facies metamorphic conditions retain their initial isotopic signature, even when associated lithologies were overprinted by greenschist- to amphibolite-facies metamorphism. Different stages of the eclogite-facies evolution can be dated provided $^{40}Ar/^{39}Ar$ dating is combined with micro-structural analyses. An age of 39 Ma from the Rote Wand – Modereck Nappe is interpreted to be close to the burial age of this unit. Eclogite deformation within the Eclogite Zone started at the pressure peak along distinct shear zones, and prevailed along the exhumation path. An age of ca. 38 Ma is only observed for eclogites not affected by subsequent deformation and is interpreted as maximum age due to the possible influence of homogenously distributed excess argon. During exhumation deformation was localised along distinct mylonitic shear zones. This stage is mainly characterised by the formation of dynamically recrystallized omphacite2 and phengite. Deformation resulted in the resetting of the Ar isotopic system within the recrystallized white mica. Flat argon release spectra showing ages of 32 Ma within mylonites record the timing of cooling along the exhumation path, and the emplacement onto the Venediger Nappe. Ar-release patterns and $^{36}Ar/^{40}Ar$ vs. $^{39}Ar/^{40}Ar$ isotope correlation analyses indicate no significant ^{40}Ar-loss after initial closure, and only a negligible incorporation of excess argon. From the pressure peak onwards, eclogitic conditions prevailed for almost 8–10 Ma.

1 Introduction

Dating of phengitic white mica provides an important tool for understanding the high-pressure evolution within an evolving orogen (e.g., Scaillet 1998), and helps to constrain early decompressional steps within a pressure-temperature-time- (PTt-) path. In contrast to other isotopic systems, e.g. Rb-Sr or Sm-Nd, the use of the ^{40}Ar and ^{39}Ar isotopes only needs one rock forming mineral for dating, despite the fact that the temperature of the Ar-isotopic system in white mica has been reported to be relatively low, and ranges from ca. 350 °C (Lips et al. 1998) to ca. 450 °C (Hames & Bowring 1994; Kirschner et al. 1996) and ca. 500 °C (Hammerschmidt & Frank 1991; Hames & Cheney 1997). Precise closure temperatures depend on grain-size, chemical composition and cooling rate. Phengitic white mica is generally predicted to have a closure temperature of about 500–550 °C, i.e. slightly higher than that of muscovite (Lister & Baldwin 1996; Stuart 2002). Furthermore, several studies (e.g. Chopin & Maluski 1980; von Blanckenburg et al. 1988, 1989; Dunlap 1997; Bossé et al. 2005) revealed, that temperature is not the only controlling mechanism for setting or re-setting the isotopic system within respective minerals (see also Villa 1998 for a general discussion). Therefore, not only the thermal, but also the tectonic history is to be investigated in detail because of the probably subordinate importance of temperature for re-setting of isotopic systems to deformation (e.g., Chopin & Maluski 1980; Handler et al. 1993; Müller et al. 1999).

In this study we dated phengitic white micas from eclogite-mylonites and their undeformed protoliths from the Eclogite Zone within the Tauern Window (Eastern Alps) (Fig. 1). From this unit a great number of PT- data are available providing a well-constrained PT- history, i.e. from subduction to subsequent exhumation. We have chosen this unit as a testing site for the combination of microstructural and geochronological studies in order to establish a well-based PTt-deformation history of the Eclogite Zone and adjacent units, and in particular the con-

[1] Institut für Erdwissenschaften, Universität Graz, Heinrichstrasse 26, A-8010 Graz, Austria.
[2] Institut für Geologie und Paläontologie, Universität Salzburg, Hellbrunner Strasse 34, A-5020 Salzburg, Austria. present address: forstinger + stadlmann ZT-OEG, Achenpromenade 14, A-5081 Anif, Austria.
[3] Institut für Mineralogie, Universität Salzburg, Hellbrunner Strasse 34, A-5020 Salzburg, Austria.
*Corresponding author: Walter Kurz. E-mail: walter.kurz@tugraz.at, walter.kurz@uni-graz.at

ditions during the exhumation of the eclogite facies rocks. A study on the microstructural evolution of these eclogites has been carried out contemporaneously in order to provide detailed knowledge about the tectono-metamorphic evolution. The results show (1) that detailed knowledge of the tectono-metamorphic history of the dated rocks provides the possibility to date both cooling following the peak of high-pressure metamorphism, and subsequent deformation in eclogites, and (2) that phengitic white micas are useful for the reconstruction of the decompressional paths in high-pressure metamorphic terranes. Inverse $^{36}Ar/^{40}Ar$ vs. $^{39}Ar/^{40}Ar$ isochrone plots prove to be useful for the detection of extraneous (excess) ^{40}Ar-components, which cannot be recognised from $^{40}Ar/^{39}Ar$ spectra, especially when dealing with relatively young rocks with rather low ^{40}Ar-content (Heizler & Harrison 1988). These diagrams are of great convenience for the recognition of atmospheric Ar and excess ^{40}Ar. The age established using an inverse isochron plot, unlike that yielded by a spectrum, is not affected by trapped $^{36}Ar/^{40}Ar$ ratios that are different from the atmospheric Ar ratio (e.g. due to excess ^{40}Ar), and may contribute to a better age interpretation.

2 Geological setting

The Eastern Alps (Fig. 1) are the product of the convergence between Africa and Europe (e.g., Frisch 1979, 1980; Neubauer et al. 2000; TRANSALP working group 2002, 2006; Schmid et al. 2004). Plate tectonic units involved in the Alpine orogen in the area of the Eastern Alps comprise (1) the European continent, represented by the Helvetic Nappes; (2) the European margin, represented by the Subpenninic Nappes (in the Tauern Window these are the Venediger Nappe, Eclogite Zone, and Rote Wand – Modereck Nappe); (3) two partly oceanic basins in the Penninic realm (the Northpenninic Valais and the Southpenninic Piemont-Liguria, represented by the Rhenodanubian Flysch, the Glockner Nappe, the Matrei Zone and the Klammkalk Zone), and (4) the Adriatic (Apulian) microcontinent including the Austroalpine and South Alpine units (Fig. 1a).

Thrusting and nappe stacking within the (Sub-) Penninic units was subsequent to south-directed subduction of the Penninic oceanic units below the Austroalpine Nappe Complex (for summary, see Kurz & Froitzheim 2002). Subsequent continental subduction of the European margin beneath the northern Adriatic continental margin commenced during the Palaeogene and resulted in thrusting of the Austroalpine nappe complex over Penninic units, and internal imbrication of the Penninic and Subpenninic nappes ("late-Alpine" orogeny, see also Kurz et al. 1998b, 2001a, b and Neubauer et al. 2000 for reviews). Thus, the Subpenninic units exposed within the Tauern Window represent the underplated European margin (Kurz et al. 2001a, b; Schmid et al. 2004; Schuster & Kurz 2005) (Fig 1b, c).

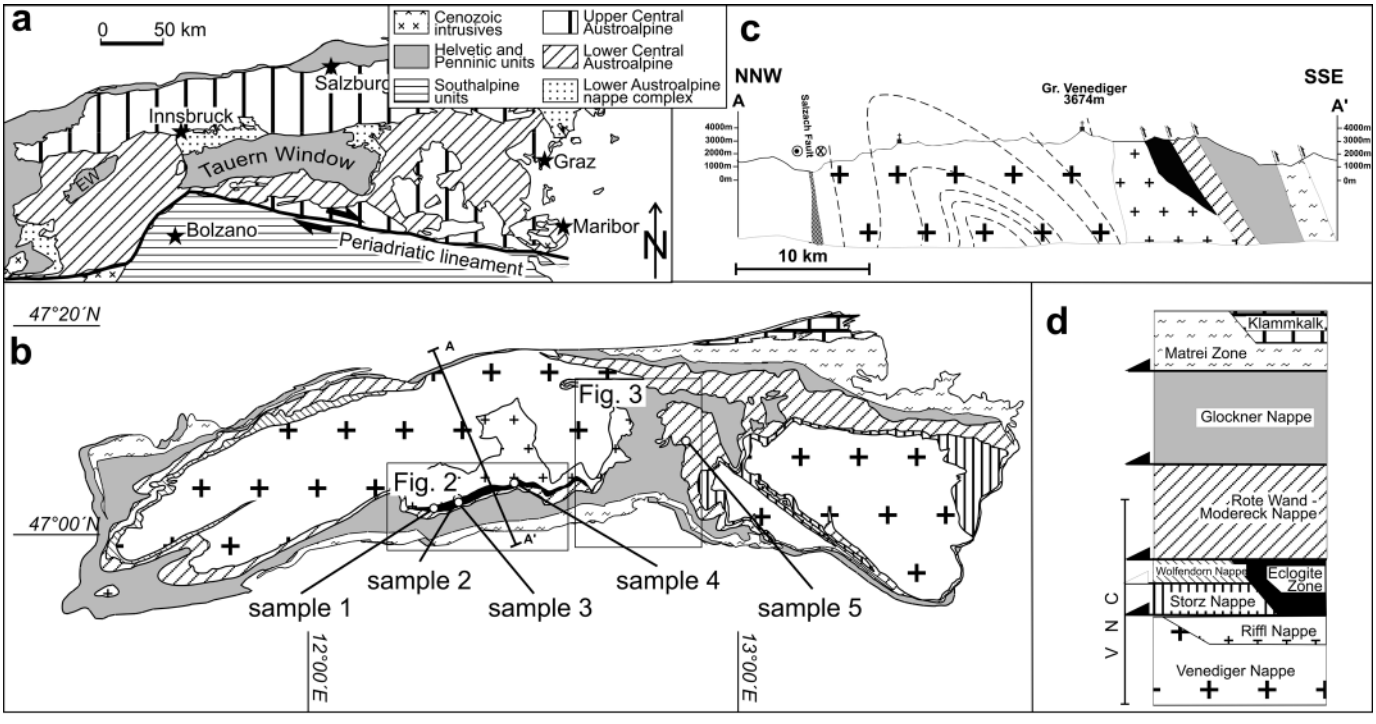

Fig. 1. (a) Simplified tectonic map, showing the major tectonic units of the Eastern Alps (after Kurz et al., 2001a); EW: Lower Engadine Window; (b) Tectonic sketch map of the Tauern Window indicating sample locations (simplified after Kurz et al. 1998a), for legend see Fig. 1d. (c) Structural section across the central Tauern Window showing the structural position of the Eclogite Zone (for location see Fig. 1b) (modified after Kurz et al., 1998a, 2001b). (d) Tectonostratigraphic sketch of the Penninic units in the Tauern Window (modified after Kurz et al. 1998b), thickness of units is not to scale.

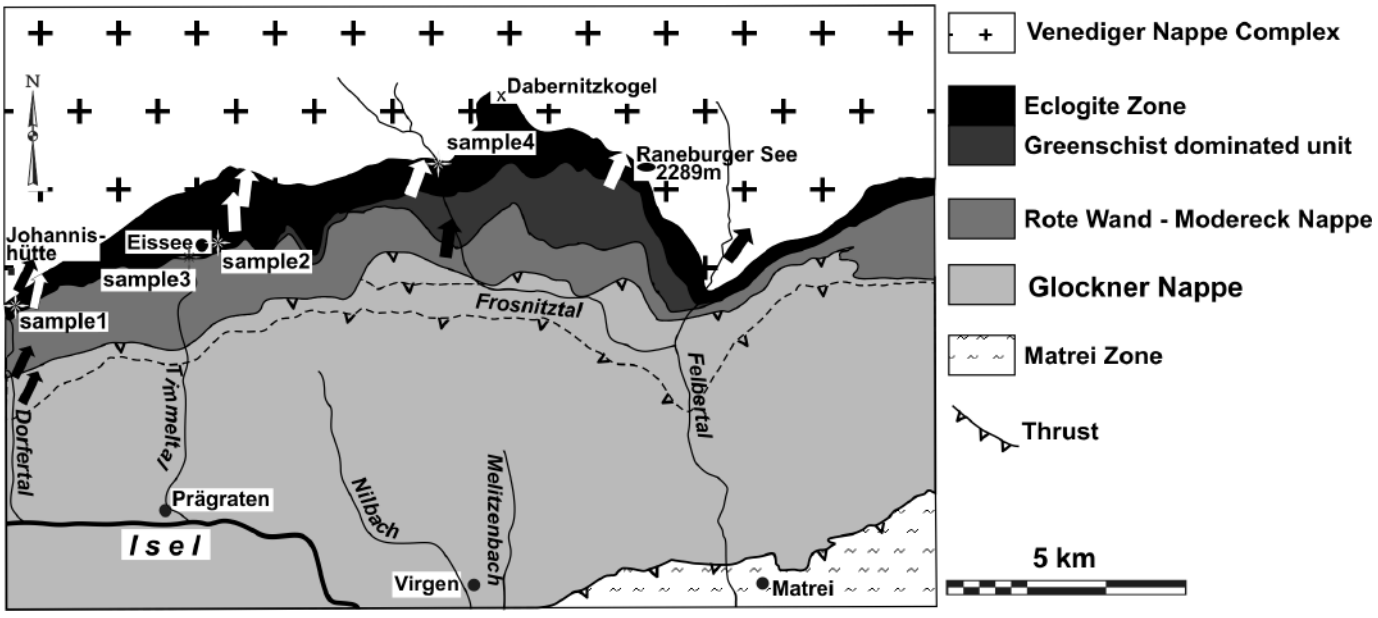

Fig. 2. Tectonic map of the central southern part of the Tauern Window, showing the structural position of the Eclogite Zone (after Kurz et al., 1998a, 2001b); the sampling sites of the eclogites used for microstructural and geochronological analysis are included; arrows indicate the kinematics of nappe emplacement of overlying units contemporaneous to HP metamorphism (D_1 in Fig. 4); the greenschist dominated unit in the upper sections of the Eclogite Zone as defined by Behrmann & Ratschbacher (1989) is characterized by almost complete retrogression of eclogites to garnet amphibolite and/or garnet-bearing greenschists. Kinematic data are available from Behrmann & Ratschbacher (1989), Kurz et al. (1996, 1998a, 2001b).

The units within the Tauern Window can be subdivided into several nappes as described in detail by Kurz et al. (1996, 1998b, 2001a). The general tectonic situation is outlined in Figs. 1b and 1c. In the area of investigation, the Eclogite Zone (Figs. 2, 3) is tectonically imbricated between the Venediger Nappe Complex below, and the Rote Wand – Modereck Nappe above. The Venediger Nappe Complex comprises the Venediger Nappe *sensu stricto*, and the Storz and Wolfendorn Nappes (Fig. 1). Lithologic similarities exist in particular between the Rote Wand – Modereck Nappe and the Eclogite Zone. Both units comprise similar sedimentary sequences of Permian to Triassic quartzites, Triassic metacarbonates and Jurassic breccias, calcareous micaschists and metatuffs. Metamorphic MORBs and gabbros, associated with metasedimentary sequences, particularly occur within the Eclogite Zone (Kurz et al. 1998b, 2001b).

3 Tectonometamorphic evolution of the Eclogite Zone and adjacent areas

The rocks exposed within the Eclogite Zone form a coherent tectonic unit (Figs. 1–3) and were affected by a multiphase tectonometamorphic evolution (for summary, see Miller 1974; Holland 1979; Raith et al. 1980; Dachs 1986, 1990; Stöckhert et al. 1997; Kurz et al. 1998a, 2004; Hoschek 2001; Kurz 2005). The Eclogite Zone is incorporated into a stack of Subpenninic nappes, overlain by the ophiolite-bearing Glockner Nappe (Figs. 1–3) and is the only tectonic unit entirely metamorphosed under eclogite-facies metamorphic conditions. The other units were only partly affected by eclogite facies metamorphism. Within garnet-micaschists, inclusions in garnet formed by paragonite + zoisite/epidote + quartz, ± phengite, chloritoide, rutile and ore minerals show rectangular to rhombohedral outlines, often interpreted as pseudomorphs after lawsonite (Dachs 1986; Spear and Franz 1986), and document a first stage of prograde metamorphism at ca. 400 °C (e.g., Frank et al. 1987). The eclogite facies rocks were buried to a depth of at least 65 km, indicated by peak pressures of 20–23 kbar at approx. 600 °C (Dachs 1986, 1990; Frank et al. 1987; Zimmermann et al. 1994; Stöckhert et al. 1997; Kurz et al. 1998a; Hoschek 2001) (Ma0 in Fig. 4). Assemblages formed along the exhumation path record approximately 15–16 kbar at 550 °C (Stöckhert et al. 1997; Kurz et al. 1998a) (Fig. 4). The Eclogite Zone was subsequently affected by blueschist facies metamorphism (Ma1 in Fig. 4). Pressures of 7–9 kbar and temperatures of ca. 450 °C are estimated by Raith et al. (1980); 450 °C and 10–15 kbar by Holland (1979) and Zimmermann et al. (1994) (Fig. 4), but the P-T data are not well constrained due to the subsequent strong overprint by amphibolite to greenschist facies metamorphism at approximately 7 kbar and 500 °C (Ma2 in Fig. 4).

For the tectonically underlying Venediger Nappe and Riffl Nappe HP metamorphism at 10–12 kbar has been determined (Selverstone et al. 1984; Cliff et al. 1985; Droop 1985; Selverstone 1993). At this metamorphic stage, corresponding to the blueschist stage of the Eclogite Zone, the Venediger nappe was incorporated into the nappe stack by top-to-the north emplacement, documented by kinematic criteria indicating a top-to-the N to NNE sense of shear both within the Eclogite Zone and in the units below and above (in particular the Venediger Nappe

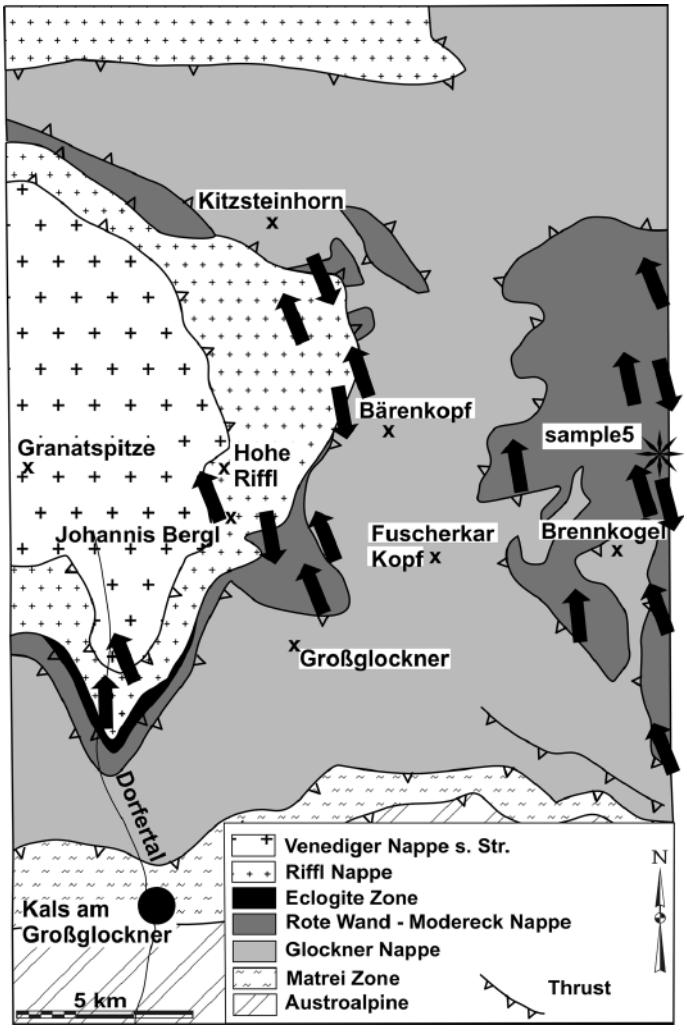

Fig. 3. Tectonic map of the central part of the Tauern Window; the sampling site of micaceous marbles used for geochronological analysis is included; arrows indicate the kinematics of nappe emplacement of overlying units during D_1, contemporaneous to HP metamorphism. Kinematic data are available from Kurz et al. (1996). Top-to-the-south kinematics is related to subsequent folding of the penetrative foliation, resulting in inversion of the shear sense.

and the Rote Wand – Modereck Nappe) (Figs. 2, 3) (D_1 in Fig. 4) (Kurz et al. 1996, 1998a, 2001b). The Venediger Nappe cooled below 300–350° C already at the end of the Oligocene, at about 23 Ma, as indicated by Rb-Sr cooling ages on biotite (e.g., Cliff et al. 1985; Droop 1985; Reddy et al. 1993).

In the units above the Eclogite Zone (i.e. the Rote Wand – Modereck Nappe and Glockner Nappe; Figs. 2, 3) remnants of eclogite facies metamorphism have been locally observed (Proyer et al. 1999; Dachs & Proyer 2001, 2002; Proyer 2003), particularly in internal sections exposed in the southern central part of the Tauern Window. In contrast to the PT- evolution of the Eclogite Zone, the Rote Wand – Modereck Nappe and the Glockner Nappe do not show blueschist facies metamorphism subsequent to the pressure peak (peak conditions of approximately 16–17 bar at 550 °C) (Dachs & Proyer 2001). After HP metamorphism, these units were affected by Barrovian-type greenschist facies metamorphism (5 kbar, 500 °C), termed "Tauernkristallisation" (e.g., Frank et al. 1987; Selverstone 1993) (Ma2 in Fig. 4).

4 Radiometric ages from the Eclogite Zone and adjacent areas

For a summary of previously published geochronological data from the Eclogite Zone see Thöni (2006). Phengite $^{40}Ar/^{39}Ar$ mineral ages of ca. 36–32 Ma (Zimmermann et al. 1994) from the Eclogite Zone were interpreted as cooling ages postdating eclogite facies metamorphism, and thus the approximate time of emplacement of the Eclogite Zone onto the Venediger Nappe under blueschist facies conditions. Ratschbacher et al. (2004) described $^{40}Ar/^{39}Ar$ ages from high-pressure amphibole, phengite, and phengite + paragonite mixtures. Combined with the thermal evolution showing nearly isothermal decompression from 25 to 15 kbar these were interpreted to document rapid exhumation through ≤15 kbar and >500 °C at ~42 Ma to ~10 kbar and ~400 °C at ~39 Ma. Assuming exhumation rates slower or equal to high-pressure–ultrahigh-pressure terrains in the Western Alps, peak pressures within the Eclogite Zone were reached not long before the high-pressure amphibole age of approx. 42 Ma (Ratschbacher et al. 2004), probably at ≤45 Ma. This is in accordance with dates from the Western Alps (e.g., Droop et al. 1990; for review see Kurz & Froitzheim 2002).

The possibility of a Palaeogene age of HP metamorphism was already discussed by Inger & Cliff (1994). Unpublished Sm-Nd garnet ages of ca. 42 Ma from the Eclogite Zone are cited by Droop et al. (1990), and Inger & Cliff (1994). Significantly younger ages of ca. 26–30 Ma are reported by Inger & Cliff (1994) for meta-sediments associated with the eclogites being penetratively affected by subsequent tectonometamorphic overprint at upper greenschist facies conditions contemporaneous to top-to-the west ductile shearing of the Penninic nappe stack (D_2 in Fig. 4). They interpret their Rb-Sr ages to date cooling of the high-pressure phengites through ca. 550 °C after crystallisation of the rocks of the Eclogite Zone. However they state that the partial resetting of the Rb-Sr isotopic system by subsequent greenschist-facies metamorphic overprint would yield ages, which have to be interpreted as mixtures between post-eclogite cooling and the greenschist overprint.

5 Eclogite microfabrics

The microstructural evolution of eclogites from the Eclogite Zone was described in detail by Kurz et al. (1998a, 2004) and Kurz (2005).

Coarse-grained boudinaged eclogites with a grain-size of up to 1 cm (Fig. 5a) may show a weak foliation (Fig. 5b). Phengite and paragonite usually do not show a preferred orientation. Omphacite shows several features of plastic deformation (D_1

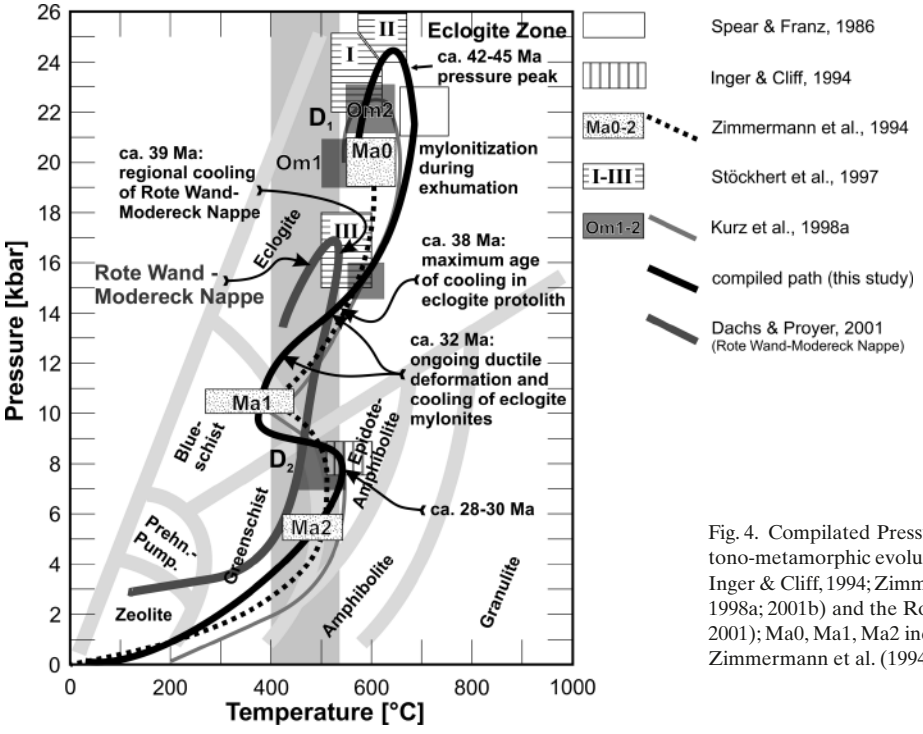

Fig. 4. Compilated Pressure – temperature – time paths, illustrating the tectono-metamorphic evolution of the Eclogite Zone (after Spear & Franz, 1986; Inger & Cliff, 1994; Zimmermann et al., 1994; Stöckhert et al., 1997; Kurz et al., 1998a; 2001b) and the Rote Wand – Modereck Nappe (after Dachs & Proyer 2001); Ma0, Ma1, Ma2 indicate events of Alpine metamorphic overprint after Zimmermann et al. (1994).

in Fig. 4). Coarse grains (omphacite1) are twinned, kinked and bent, and show undulatory extinction and the formation of subgrains (Fig. 5a, b). The subgrain boundaries are generally oriented subparallel to the prism planes. With increasing degree of deformation, the long axes of the subgrains are preferentially oriented subparallel to the trace of the foliation and lineation in XZ- sections (Fig. 5b). Fine grains of recrystallized omphacite (omphacite2) are formed along the grain boundaries of coarse omphacite (omphacite1) (Fig. 5a). Omphacite1 is characterized by jadeite contents of approx. 30 mol%, omphacite2 by jadeite contents of approx. 50 mol% (Kurz et al. 1998a). Omphacite1 is chemically (and optically) zoned (Fig. 5a); the cores and the rims show jadeite contents of approx. 25 mol% and 30–35 mol%, respectively (Kurz et al. 1998a, 2004). Thermobarometric data indicate conditions of 17–20 kbar at approx. 550–580 °C during the formation of omphacite1 (Om1 in Fig. 4), and 20–23 kbar at 600–620 °C at the pressure peak during the formation of omphacite2 (Om2 in Fig. 4) (for details see Kurz et al. 1998a). Therefore, the deformational fabrics document the final section of the prograde evolution up to the pressure peak.

Several stages from coarse-grained eclogites to the formation of fine-grained eclogite mylonites with dynamically recrystallized omphacite2 have been observed. Strongly foliated eclogitic mylonites show a well-developed mylonitic foliation and a stretching lineation defined by elongate garnet, omphacite2, zoisite, kyanite, and glaucophane. Locally, a compositional layering of single-grain-thick quartz layers, garnet, and omphacite is developed. Within the fine-grained mylonites, omphacite2 shows an elongated shape and a shape preferred orientation subparallel to the penetrative mylonitic foliation (Fig. 5c). Synkinematic phengites are tightly arranged parallel to the penetrative foliation. Glaucophane and barroisitic hornblende, having been formed along the decompressional path, but still under eclogite facies metamorphic conditions (Kurz et al. 1998a), occur in several of the fine-grained, omphacite2 dominated eclogites. Omphacite2 is also partly replaced by these types of amphibole along its rims (Fig. 5d).

The garnet grains are characterized by a round, inclusion-rich core and inclusion-free rims. The grains show straight boundaries and a hypidiomorphic shape (Fig. 5b, c). Garnet is often enriched within monomineralic layers. Within fine-grained mylonites, many garnets show an elongated shape (Fig. 5c), and a shape preferred orientation parallel to the lineation direction, resulting from preferential growth parallel to the kinematic x-axis (Kurz et al. 2004).

From the microstructures and radiometric data described above, the following distinct episodes along the PT- path of the Eclogite Zone can be reconstructed:

1. Deformation at peak pressure conditions indicated by the analysis of microstructures and geothermobarometric data (for details, see Stöckhert et al. 1997; Kurz et al. 1998a, 2004; Kurz 2005) (Fig. 4).
2. Distinct overprints along the decompression path, including a blueschist facies metamorphic overprint; evidence is provided by the analysis of microstructures and geothermobarometric data (for details, see Stöckhert et al. 1997; Kurz et al. 1998a, 2004).

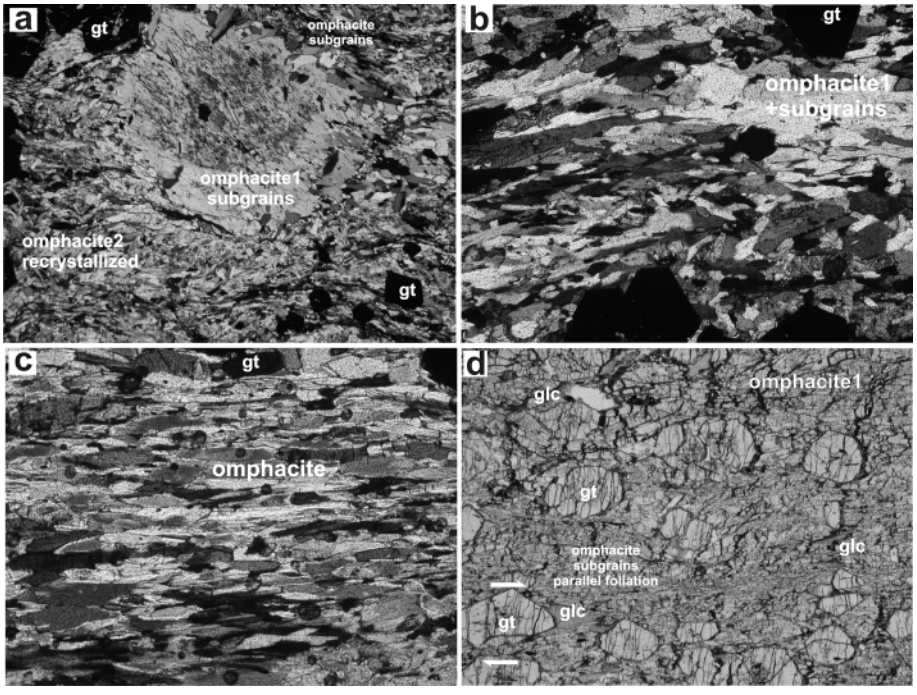

Fig. 5. Microstructures of eclogites from the Eclogite Zone (Tauern Window) (for sample locations see Fig. 2 and the Appendix). a – XZ-section of coarse-grained, un-foliated eclogite, showing omphacite1 with subgrains, and dynamically recrystallized omphacite2 grains along its rim; subgrain boundaries are subparallel to the traces of {010}. b XZ- section of coarse-grained foliated eclogite showing remnants of omphacite1, surrounded by fine-grained dynamically recrystallized omphacite2. c – XZ section of eclogite mylonite showing dynamically recrystallized omphacite2 with well-developed shape preferred orientation in XZ. d – XZ- section of eclogite mylonite showing dynamically recrystallized omphacite2 and glaucophane with well developed shape preferred orientation in XZ; glaucophane is partly replacing omphacite2 and has been formed subsequent to the pressure peak, probably at the transition from eclogite to blueschist facies metamorphism. a, b, c: Crossed polarized Nicols; a–d: long axis of photograph about 4 mm; gt: garnet.

3. Cooling through the closure temperature for the Ar isotopic system of white mica (assumed to lie between 400 °C and 550 °C) (Fig. 4).

The segment between the pressure peak and the cooling through the Ar closure temperature in white mica is less constrained and will be discussed by providing new $^{40}Ar/^{39}Ar$ mineral ages.

6 Samples analysed by $^{40}Ar/^{39}Ar$ stepwise heating

The sample sites of analysed eclogites are all located in the northern (internal) part of the Eclogite Zone (see Figs. 1–3 and Appendix), outside the greenschist dominated unit described by Behrmann & Ratschbacher (1989) (Fig. 2). Two types of eclogite samples, not overprinted by subsequent greenschist-amphibolite facies metamorphic assemblages, have been investigated for the presented study: (1) Eclogite-mylonites (samples 1–3) with syn-kinematically grown phengite; the typical mineral assemblage of these samples is shown in Figs. 6a, b, and comprises garnet, omphacite2 (Fig. 4), zoisite, glaucophane, kyanite, phengite, and quartz. Estimates on the PT-conditions for eclogite-facies metamorphism are provided by Kurz et al. (1998a) (Fig. 4) (20–23 kbar, 600–620 °C for the peak assemblage) (eclogite mylonites containing omphacite2, but lacking glaucophane and barroisitic hornblende). (2) Samples of unfoliated fine-grained eclogite (sample 4) (Fig. 6c), not affected by deformational overprint subsequent to the pressure peak, but occurring together with foliated eclogite mylonites, were analysed for comparison. The eclogite facies mineral assemblage comprises garnet, omphacite1 (Fig. 4), kyanite, quartz, paragonite and subordinate phengite. Estimates on the PT-conditions for eclogite-facies metamorphism are provided by Kurz et al. (1998a) (Fig. 4) (18–20 kbar at 530–570 °C for unfoliated eclogites containing omphacite1).

Additionally, a calcite-marble (sample 5) (Fig. 6d) from the Rote Wand – Modereck Nappe (for location see Fig. 3) has been analysed to get information on the cooling history of the unit immediately above the Eclogite Zone, because geothermobarometric studies have satisfactorily shown eclogite facies metamorphism in parts of this unit as well (ca. 550 °C, 15 kbar) (Dachs & Proyer 2001). The location indicated in Fig. 3 has been chosen, because this area shows low degree of metamorphic and deformational overprint under greenschist facies conditions (D_2 in Fig. 4). This should therefore provide an undisturbed original Ar isotopic composition related to the peak metamorphic conditions.

Samples 1–3 are characterised by similar microstructures, showing a strong penetrative mylonitic foliation with a shape preferred orientation of omphacite2 (with an average grain size of 100–250 µm), zoisite, glaucophane, and phengite (Fig. 6a, b), corresponding to the microstructures of fine-grained eclogite mylonites described above (Figs. 5b, c). Phengites reach a grain size of up to 500 µm. Sample 4 shows a less developed shape preferred orientation compared to previously described samples (Fig. 6c), indicating that penetrative ductile deformation in this sample was less pronounced. Grain-size ranges from 10 to 50 µm, only white mica reaching a grain size of up to 250 µm. The microstructures are indicative for coarse- to medium-grained eclogites described above (Fig. 5a). Although most of the associated lithologies were affected by later retrogression

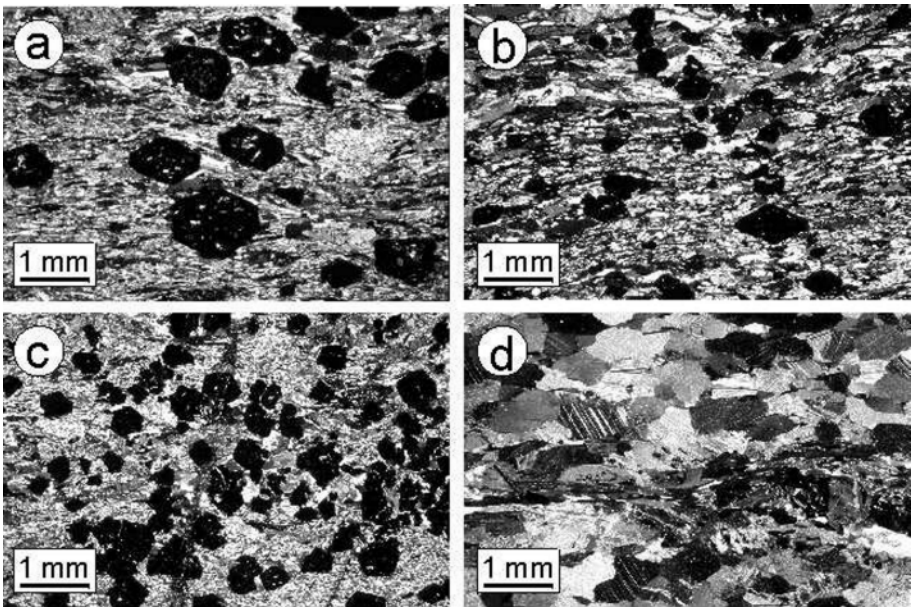

Fig. 6. Examples of typical microstructures of the dated samples. a, b – Eclogite-mylonite samples 1 and 2 indicate strong shape-preferred orientation of phengite, and recrystallized omphacite. Note also the intense elongation of garnet (with an aspect ratio of up to 1.8). c – By contrast, the fine-grained eclogite sample 4 indicates no characteristics for ductile deformation and equidimensional garnet textures. d – Calcite marble sample 5 indicates a penetrative foliation, which is traced by layers of white mica.

at amphibolite to greenschist facies metamorphic conditions, all the eclogite samples described in this study were preserved as meta-stable assemblages, most probably related to the absence of fluids in these rock domains. Sample 5 (Fig. 6d) has been taken from a calcite-marble near the structural base of the Rote Wand – Modereck Nappe. Retrogressed eclogites, intercalated with these marbles, show relics of high-pressure assemblages (Proyer et al. 1999; Dachs & Proyer 2001). Within the marbles the penetrative foliation is traced by layers of white mica sporadically accumulated along isolated foliation (i.e. former bedding) planes.

7 Results

7.1 Electron microprobe analysis

Between 10–20 electron microprobe analyses have been carried out on white mica concentrates of samples 1–5. The chemical formulae for white mica were calculated on the basis of 56 cation charges. Average mica compositions are listed in Table 1 and graphically presented in a muscovite –50% celadonite – paragonite plot (Fig. 7). Analyses are discussed with respect to their muscovite (Ms), celadonite (Cel), paragonite (Pg), and margarite (Mrg) components.

White micas from eclogite-mylonite samples (1A, 1B, 2, and 3) are phengites with similar chemical compositions (average ca. $Ms_{40}Ce_{51}Pg_{9}$). Both size-fractions of sample 1 (1A: 200–250 µm; 1B: 250–355 µm) yielded similar compositions. White micas from the fine-grained eclogite sample 4 are paragonites with an average composition of $Ms_5Pg_{93}Mrg_2$. White micas from calcite marble (sample 5) have a slightly less phengitic composition than eclogite-mylonite samples 1–3, with an average of ca. $Ms_{64}Cel_{32}Pg_4$.

7.2 $^{40}Ar/^{39}Ar$ dating

$^{40}Ar/^{39}Ar$ analyses have been carried out on six different white mica multi-grain concentrates (ca. 15 grains per sample) of five samples. A detailed description of the analytical techniques and procedures can be found in Handler et al. (2004).

Analytical results are portrayed as age spectra in Fig. 8 together with $^{36}Ar/^{40}Ar$ vs. $^{39}Ar/^{40}Ar$ isotope correlation plots. The detailed analytical results can be requested from the publisher and are provided in the electronic version.

From sample 1 two size fractions (1A: 200–250 µm, and 1B: 250–355 µm) have been analysed. The Ar-release spectrum of sample 1A displays a nearly flat pattern, indicating homogeneous Ar-isotopic composition released through the experiment, and pointing to an undisturbed Ar-isotopic composition of the white mica. Age calculation over all increments yielded

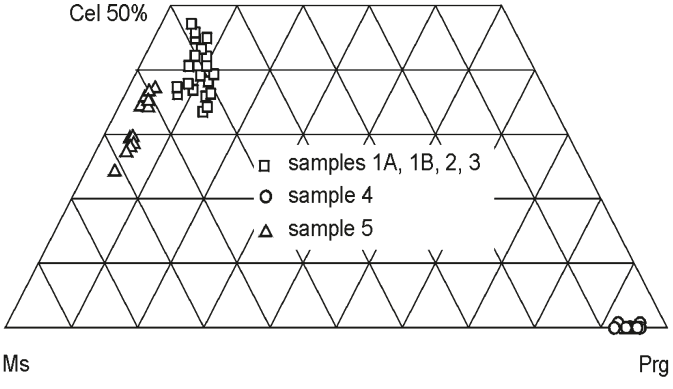

Fig. 7. Muscovite (Ms) –50% Celadonite (Cel) – Paragonite (Prg) triangle-plot of chemical composition of white-mica samples 1–5 analysed by electron microprobe. Each data point represents one individual grain mounted on carbon glass slides.

Table 1. Microprobe analyses of white mica from eclogite samples 1–4, and calcite-marble sample 5 of the Tauern Window, Eastern Alps (Austria). Ms = Muscovite, Pg = Paragonite, Mrg = Margarite (following suggestions of KRETZ, 1983), Cel = Celadonite; n = number of analysis on the sample; <3σ = below detection limit of 3σ; values in parentheses are 1σ standard deviation.

	Sample 1A	Sample 1B	Sample 1A + 1B	Sample 2	Sample 3	Sample 4	Sample 5
n	5	16	21	18	12	15	14
SiO2	49.88 (86)	50.81 (99)	50.53 (99)	50.10 (99)	50.69 (90)	46.28 (52)	49.40 (99)
Al2O3	27.15 (26)	27.45 (57)	27.41 (50)	26.70 (70)	27.13 (50)	39.29 (51)	29.50 (60)
TiO2	0.29 (02)	0.28 (04)	0.28 (04)	0.28 (07)	0.26 (03)	0.07 (02)	0.30 (16)
FeO	1.59 (07)	1.55 (07)	1.56 (08)	2.20 (30)	1.90 (15)	0.47 (04)	0.80 (11)
MgO	3.61 (08)	3.65 (18)	3.60 (16)	3.40 (30)	3.43 (20)	0.15 (05)	2.90 (20)
MnO	<3σ	<3σ	<3σ	<3σ	<3σ	<3σ	<3σ
K2O	9.87 (36)	10.13 (21)	10.10 (30)	10.40 (20)	10.20 (13)	0.64 (15)	10.80 (11)
Na2O	0.81 (13)	0.73 (13)	0.70 (13)	0.60 (14)	0.67 (06)	7.36 (26)	0.32 (04)
CaO	<3 σ	<3 σ	<3 σ	<3 σ	<3 σ	0.32 (04)	<3 σ
Total	93.19	94.59	94.18	93.68	94.28	94.57	94.02
Si	6.77 (05)	6.79 (06)	6.79 (05)	6.81 (07)	6.82 (04)	5.97 (02)	6.64 (08)
Al(tot)	4.35 (04)	4.33 (07)	4.34 (07)	4.27 (06)	4.30 (06)	5.97 (04)	4.68 (11)
Ti	0.03 (00)	0.03 (00)	0.03 (00)	0.03 (01)	0.03 (00)	0.01 (00)	0.03 (02)
Mg	0.73 (02)	0.73 (04)	0.72 (04)	0.69 (05)	0.69 (04)	0.03 (01)	0.58 (04)
Fe	0.18 (01)	0.17 (01)	0.18 (01)	0.25 (03)	0.21 (01)	0.05 (00)	0.09 (01)
Mn	<3σ	<3σ	<3σ	<3σ	<3σ	<3σ	<3σ
K	1.71 (07)	1.73 (05)	1.73 (05)	1.80 (05)	1.75 (04)	0.11 (02)	1.85 (03)
Na	0.21 (04)	0.19 (04)	0.18 (04)	0.16 (04)	0.17 (02)	1.84 (07)	0.08 (01)
Ca	<3σ	<3σ	<3σ	<3σ	<3σ	0.04 (01)	<3σ
Cel	38.58 (2.30)	39.70 (2.83)	39.48 (2.74)	40.30 (3.55)	40.85 (1.99)	–	32.16 (3.89)
Ms	50.45 (1.39)	50.50 (1.32)	50.99 (1.34)	51.64 (2.55)	50.08 (1.49)	5.29 (1.20)	63.53 (3.58)
Pg	10.96 (1.46)	9.80 (1.79)	9.53 (1.78)	8.06 (1.87)	9.08 (0.81)	92.49 (1.02)	4.31 (0.54)
Mrg	–	–	–	–	–	2.22 (0.31)	–

an age of 32.5 ± 0.15 Ma. The $^{36}Ar/^{40}Ar$ vs. $^{39}Ar/^{40}Ar$ isotope correlation plot yields a y-axis intercept of $^{36}Ar/^{40}Ar = 0.00310$ (MSWD = 9.6). Because this value is comparable to the present day atmospheric composition of Ar ($^{36}Ar/^{40}Ar_{atm} = 0.00338$), we conclude that no excess Ar has been incorporated at or after the time of initial closure of the isotopic system in these micas.

The coarser grained phengite (sample 1B) indicates slightly higher ages in the first three low-temperature gas release steps, pointing either to optically undetectable intergrowths with higher Ar-retention, or minor influx of extraneous ^{40}Ar-components. Similar ages as for sample 1A are obtained from further steps of the Ar-release pattern (steps 4–13, together comprising 90.3% of the total ^{39}Ar released) (33.3 ± 0.15 Ma). Minor incorporation of excess ^{40}Ar-components is also indicated by the $^{36}Ar/^{40}Ar$ vs. $^{39}Ar/^{40}Ar$ isotope correlation plot, where the ratios of the first three increments define a trend-line, which clearly points to a $^{36}Ar/^{40}Ar$ intercept, being much lower than atmospheric composition. Therefore, a regression line has been calculated only for steps 4–13, which define a plateau in the Ar-release spectrum. The isotope correlation analysis of these steps yielded a y-axis intercept of $^{36}Ar/^{40}Ar = 0.00347$ (MSWD = 0.66), close to the atmospheric Ar-composition.

White mica of sample 2 has the same grain-size (250–355 µm) as sample 1B described above. The Ar-release plot displays fairly consistent ages, except for the first increment, which again displays a slightly older age. Calculation over steps 2–13, together comprising 99.1% of the total ^{39}Ar released, yielded an age of 32.5 ± 0.15 Ma. Regression analyses over these steps within the $^{36}Ar/^{40}Ar$ vs. $^{39}Ar/^{49}Ar$ isotope correlation plot yields a y-axis intercept of $^{36}Ar/^{40}Ar = 0.00309$ (MSWD = 2.6).

For sample 3 coarse-grained (250–355 µm) white micas have been analysed as well. The Ar-release plot displays a flat age spectrum, indicating no disturbance after initial closure of the Ar-isotopic system. Age calculation over all increments yielded 31.8 ± 0.15 Ma, the $^{36}Ar/^{40}Ar$ vs. $^{39}Ar/^{40}Ar$ isotope correlation plot yields a y-axis intercept of $^{36}Ar/^{40}Ar = 0.00289$ (MSWD = 11.7).

White mica sample 4 (200–250 µm) has been separated from a fine-grained eclogite. The Ar-release plot again displays a flat spectrum; only the first step yields a slightly older age. The 1σ error range for this analysis is rather wide related to the low K- content of the analysed paragonite, resulting in low Ar- contents (see Table 1). The total-gas age of this sample is 38.0 ± 0.55 Ma. The regression line of the $^{36}Ar/^{40}Ar$ vs. $^{39}Ar/^{40}Ar$ isotope correlation plot yields a y-axis intercept of $^{36}Ar/^{40}Ar = 0.00329$ (MSWD = 0.53).

White mica sample 5 (250–355 µm) has been separated from a calcite-marble of the Rote Wand – Modereck Nappe. The Ar-release plot displays a slightly disturbed age spectrum. However, the total-gas age of 39.00 ± 0.15 Ma is comparable to the results of sample 4. The regression line calculated

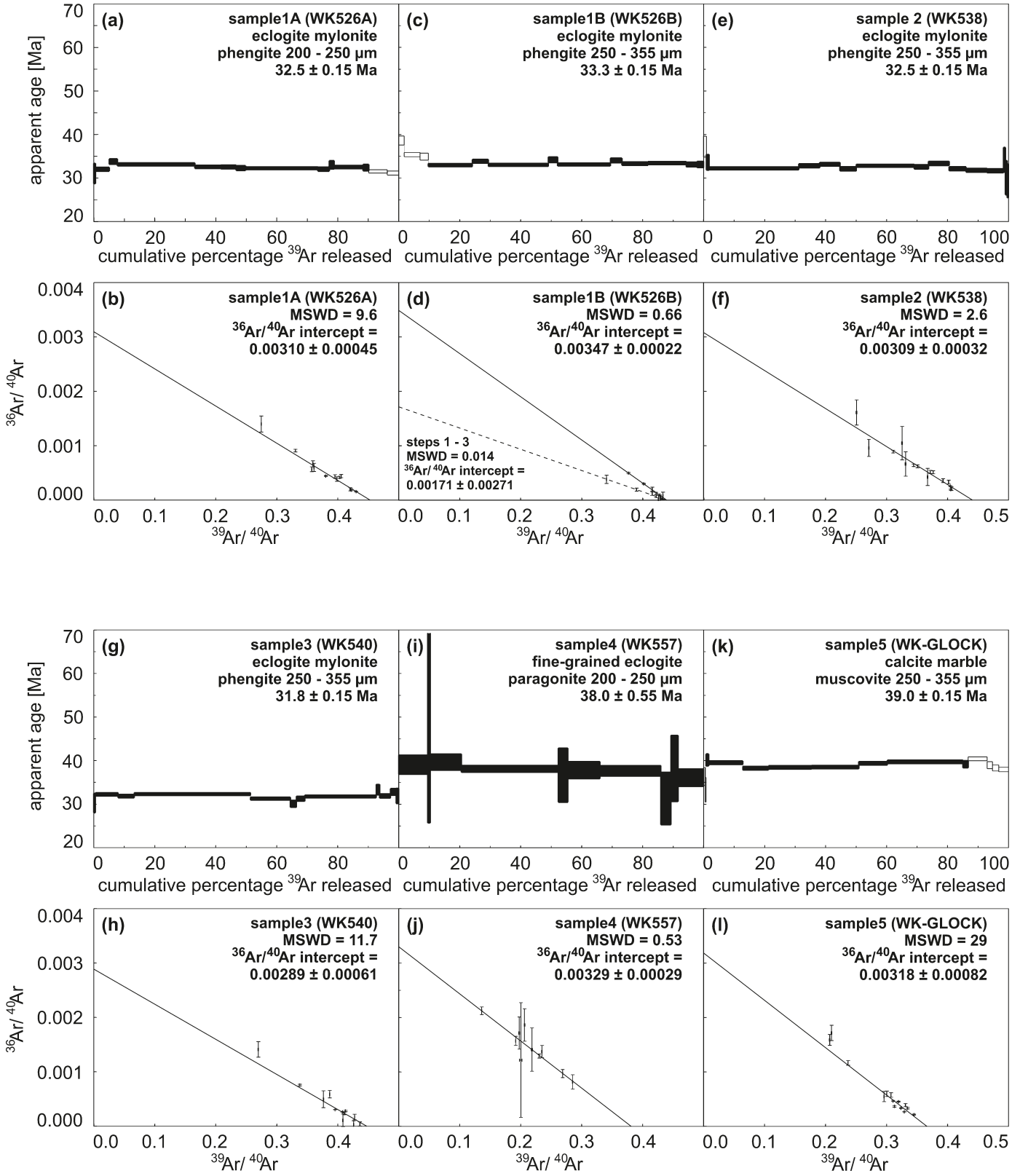

Fig. 8. $^{40}Ar/^{39}Ar$ age spectra and related $^{36}Ar/^{40}Ar$ vs. $^{39}Ar/^{49}Ar$ isotope correlation plots of white mica multi-grain analyses from the Eclogite Zone and the Rote Wand – Modereck Nappe of the Tauern Window; intensity of the laser increases from left to right; increments used for age calculation are indicated; analytical errors (1-sigma) are given by vertical width of bars; half length of error bars in isotope correlation plots indicates 1 sigma error.

over all increments in the $^{36}Ar/^{40}Ar$ vs. $^{39}Ar/^{40}Ar$ isotope correlation plot yields a y-axis intercept of $^{36}Ar/^{40}Ar = 0.00318$ (MSWD = 29).

7.3 Data quality

Analyses of white micas from eclogite mylonites (samples 1–3) display flat Ar-release spectra with ages ranging between 31.8 ± 0.15 Ma and 33.3 ± 0.15 Ma. Only two of four Ar-release plots display slightly older ages in the first increments (samples 1B, and 2), suggesting minor influx of excess ^{40}Ar-components. When these increments are not taken into account, regression analyses of the $^{36}Ar/^{40}Ar$ vs. $^{39}Ar/^{40}Ar$ isotope correlation plots yield y-axis intercepts ranging between $^{36}Ar/^{40}Ar = 0.00289$ and $^{36}Ar/^{40}Ar = 0.00347$ for all four analyses, being fairly close to the atmospheric isotopic composition of $^{36}Ar/^{40}Ar = 0.00338$. There is no correlation between the age of the samples and the extrapolated $^{36}Ar/^{40}Ar$ ratio. Furthermore, analysis of sample 1A indicates a perfectly flat Ar-release pattern and an extrapolated $^{36}Ar/^{40}Ar$ ratio nearly identical to the atmospheric value. We therefore conclude that the different ages reported in samples 1–3 do not indicate incorporation of significant amounts of excess ^{40}Ar-components in the Ar-system.

Sample 4, separated from an un-foliated eclogite, and sample 5, separated from a calcite-marble of the Rote Wand – Modereck Nappe display significantly older ages compared to the mylonitic eclogites (samples 1–3). Integrated ages are 38.0 ± 0.55 Ma and 39.00 ± 0.15 Ma, respectively. The relatively large age-error for sample 4 results from the low K- and, therefore, Ar-content of the analysed paragonites. We do not observe any correlation between ages, grain-size within eclogite mylonites, and extrapolated $^{36}Ar/^{40}Ar$ ratios. The $^{36}Ar/^{40}Ar$ vs. $^{39}Ar/^{40}Ar$ isotope correlation plot of sample 4 yields a y-axis intercept of fairly atmospheric composition. In the $^{36}Ar/^{40}Ar$ vs. $^{39}Ar/^{40}Ar$ isotope correlation plot of sample 5 the y-axis intercept yields at 0.00318, which may indicate minor incorporation of an excess ^{40}Ar-component. However, the first two steps of the Ar-release spectrum of this sample indicate Ar-loss rather than incorporation of ^{40}Ar. Therefore, the integrated age is interpreted to be geologically meaningful, and the age difference of ca. 7 Ma between white micas separated from eclogite-mylonites (samples 1–3) and white micas separated from calcite marbles (sample 5) to be significant.

8 Discussion and geological implications

The new radiometric ages presented in this study show that phengites formed under eclogite-facies metamorphic conditions retain their isotopic signature, even when associated lithologies were affected by greenschist- to lower amphibolite-facies metamorphic overprint. Despite a few domains showing distinct retrogression to (garnet-) amphibolites, most of the eclogites within the Eclogite Zone were preserved, showing their eclogite facies mineral assemblages. This may be explained in several ways:

1. The Eclogite Zone was exhumed at very high exhumation rates (for discussion, see Glodny et al. 2005) and, therefore, subsequent metamorphic overprint by conductive heat transfer was either prevented or delayed (e.g. Ernst 2006).
2. Subsequent metamorphism proceeded at conditions of heterogeneous fluid distribution, documented by the adjoining occurrence of both well-preserved and completely retrogressed eclogites, and the occurrence of hydrothermal veins.
3. Ongoing deformation under eclogite facies conditions.

Resetting of the Ar-isotopic system during exhumation was highly influenced by concomitant ductile deformation in terms of mylonitization, and heterogeneous regional fluid flow. This is supported by observations and theoretical considerations of previous workers (e.g. Chopin & Maluski 1980; von Blanckenburg et al. 1989; 1993; Villa 1998) that in certain cases ductile deformation is of greater importance for the resetting of isotopic systems than temperature. Furthermore our study shows that different stages of an eclogite-facies metamorphic event can be dated when $^{40}Ar/^{39}Ar$ dating is combined with microstructural investigations.

The ages presented in this study are in accordance with previously published phengite $^{40}Ar/^{39}Ar$ mineral ages from the Eclogite Zone of ca. 36–32 Ma (Zimmermann et al. 1994). These were interpreted as cooling ages postdating eclogite facies metamorphism, and thus taken to date the approximate time of emplacement of the Eclogite Zone onto the Venediger Nappe. Similarly, Ratschbacher et al. (2004) described $^{40}Ar/^{39}Ar$ ages from high-pressure amphibole (ca. 42 Ma), phengite, and phengite+paragonite mixtures (ca. 39 Ma). Based on our new data, we can draw some additional constraints on the available PTt-paths of the Eclogite Zone and adjacent units (Fig. 4). Related to the observed microstructures, deformation at eclogite facies conditions started close to the pressure peak, documented by the formation of dynamically recrystallized omphacite2 (Fig. 5) (Kurz et al. 1998a, 2004), and the synkinematic crystallisation of phengite. Omphacite2 and phengite are present in equilibrium and formed syndeformatively. Inevitably, the pressure peak marks the transition from subduction-related burial to exhumation (Kurz 2005). Deformation was localised mainly along distinct shear zones, and prevailed along the exhumation path (Fig. 4). During decompression and cooling the Ar-isotopic system was initially closed at ca. 38 Ma. These ages are only observed for rocks not affected by subsequent deformational and metamorphic overprint. The Ar release spectra show that the Ar-isotopic system in these white micas was slightly affected by incorporation of excess ^{40}Ar-components or Ar-loss after initial closure. The dated paragonite within these rocks, generally showing a lower closure temperature compared to phengite, is very sensitive for excess Ar. Due to the low K content and the young age only a low amount of excess Ar may have a large influence on the age. Therefore, this age is interpreted as maximum cooling age of the previously established eclogite-facies metamorphic assemblage. Although the isotope correlation

plots do not show any influence of excess Ar from an external source (Kelley 1995), and therefore show an atmospheric composition, it is not possible to determine Ar which was set free in the same rock volume above the closure temperature and caught to an undefined amount later on, when the rock passes through the closure window. This may happen when there is only very restricted fluid flow, which may also be responsible for the metastable preservation of peak metamorphic assemblages. Especially a homogeneous distribution of radiogenic excess Ar cannot be detected. Accordingly, the ages provided by paragonite from undeformed eclogites (38 Ma) are approximately 5–6 Ma older than the ages within the mylonite.

From the pressure peak onwards deformation in the eclogite-mylonites (samples 1–3) continued under eclogite-facies conditions along the exhumation path; this is indicated by the synkinematic replacement of omphacite by glaucophane as well. Shear localisation, causing strain softening, resulted in the dynamic recrystallization of white mica within the mylonites. The phengite analyses display flat Ar-release spectra, irrespective of the white mica grain size. Only two of four Ar-release plots display slightly older ages in the first increments (samples 1B, and 2), suggesting minor influx of excess ^{40}Ar-components. This indicates a quite homogenous Ar-retention.

Both types of eclogites analysed (deformed and undeformed), do not show any indication of subsequent overprint by greenschist to amphibolite facies metamorphic mineral assemblages, but show similar sizes of the major rock-forming minerals (garnet, omphacite). This additionally suggests that the different ages may not be attributed to the average grain size of the host rock in terms of intergranular diffusion rates, and not to different grade of metamorphic overprint, but either to deformation enhanced resetting of the Ar-isotopic system, or to homogenously distributed small amounts of excess Ar within paragonite in undeformed samples.

The close relationship between microstructural observations and geochronological ages documents that in samples free of predeformative relics an assemblage in isotopic equilibrium has been frozen during syn-deformational cooling (Glodny et al., 2008). Therefore, the flat Ar release spectra showing ages of 32 Ma within omphacite2- mylonites record the timing of exhumation, with an upper closure temperature limit of up to 550 °C (Hammerschmidt & Frank 1991; Hames & Bowring 1994; Kirschner et al. 1996; Hames & Cheney 1997) (550 °C particularly for phengite). The Rb-Sr ages of approximately 32 Ma presented by Glodny et al. (2005) can therefore be interpreted on this note as well. Referring to exhumation-related assemblages, indicating conditions of 15–16 kbar at approx. 550 °C (Fig. 4) (Stöckhert et al. 1997; Kurz et al. 1998a), the ages of samples 1–3 indicate decompression through 15 kbar at 32 Ma.

Later these rocks experienced a greenschist to amphibolite facies metamorphic overprint at 525 °C and 7,5 kbar (Dachs 1990). The metamorphic temperatures are quite close to the upper closure temperature limit of the Ar-system in phengite, but may have been too low to cause complete Ar resetting. Ages in the range of 28–30 Ma published by Inger & Cliff (1994) can be interpreted in terms of subsequent resetting; however, these ages are from associated meta-sedimentary sequences, mainly situated within the greenschist dominated unit (Fig. 2). Rb-Sr ages of pseudomorphs of lawsonite from this area (Gleissner et al. 2007), situated within the Glockner Nappe, show that the decomposition of lawsonite occurred at 30 Ma and are interpreted to reflect the onset of greenschist facies metamorphic overprint, just following the final exhumation of the Eclogite Zone. This might indicate that the age of 32 Ma is a cooling age very close to the beginning of thermal overprint.

Sm-Nd garnet ages of ca. 42 Ma from the Eclogite Zone (see Droop et al. 1990, Inger & Cliff 1994), and recently published ^{40}Ar/^{39}Ar ages of ca. 39–42 Ma from high-pressure amphibole, phengite, and phengite+paragonite mixtures (Ratschbacher et al. 2004) may be used to constrain the timing of peak conditions during eclogite facies metamorphism and subsequent cooling, and therefore the formation of omphacite1-bearing eclogites. These ages are quite similar to the Sm-Nd garnet ages and U-Pb SHRIMP ages reported for units of a comparable tectonic position in the Central and Western Alps (e.g. Dora Maira, Adula Nappe) (for summary, see Kurz & Froitzheim 2002). By combining our new data with the previously published ages, we suggest the following tectonic evolution of the Eclogite Zone and associated tectonic units within the Tauern Window (Fig. 9), based on the PTt evolution shown in Fig. 4:

The oceanic lithosphere preserved in the Glockner Nappe was subducted during the Late Cretaceous to Eocene (Fig. 9a), with parts of it reaching eclogite facies metamorphism. Subsequently, the European margin descended into the subduction zone, resulting in eclogite facies metamorphism in the Eclogite Zone at about 40–42 Ma (Fig. 9b). The Eclogite Zone ascended towards the surface within the subduction channel (Kurz et al. 1998a; Kurz & Froitzheim 2002; Kurz 2005), while subduction was still active and, hence, heating was prevented (Kurz et al. 1998a, b; 2001b; Kurz & Froitzheim 2002). This is evidenced by cooling during decompression and the subsequent blueschist facies metamorphic overprint (Fig. 4). An age of ca. 38 Ma from undeformed eclogites is assumed to be a maximum age of this cooling event. Cooling of the Rote Wand – Modereck Nappe occurred approximately at the same time (39 Ma). As the peak temperatures during HP metamorphism within the Rote Wand – Modereck Nappe (ca. 550 °C at 15–16 kbar; Dachs & Proyer 2001) are near to the closure temperature for the Ar system in phengite, this age (39 Ma) is interpreted to be close to the burial age of this unit, and therefore of the European margin. Accordingly, the pressure peak within the Eclogite Zone, originally situated south of the Rote Wand – Modereck Nappe (Kurz et al. 1998b) (Fig. 9b) was reached contemporaneously or slightly before, as indicated by the ages (39–42 Ma) published by Ratschbacher et al. (2004). Syndeformational cooling, related to the emplacement of the Eclogite Zone onto the Venediger Nappe, and the subsequent emplacement of the Rote Wand – Modereck Nappe along a major out-of-sequence detachment above at mid- to lower crustal levels (Fig. 9c, d), may be dated at

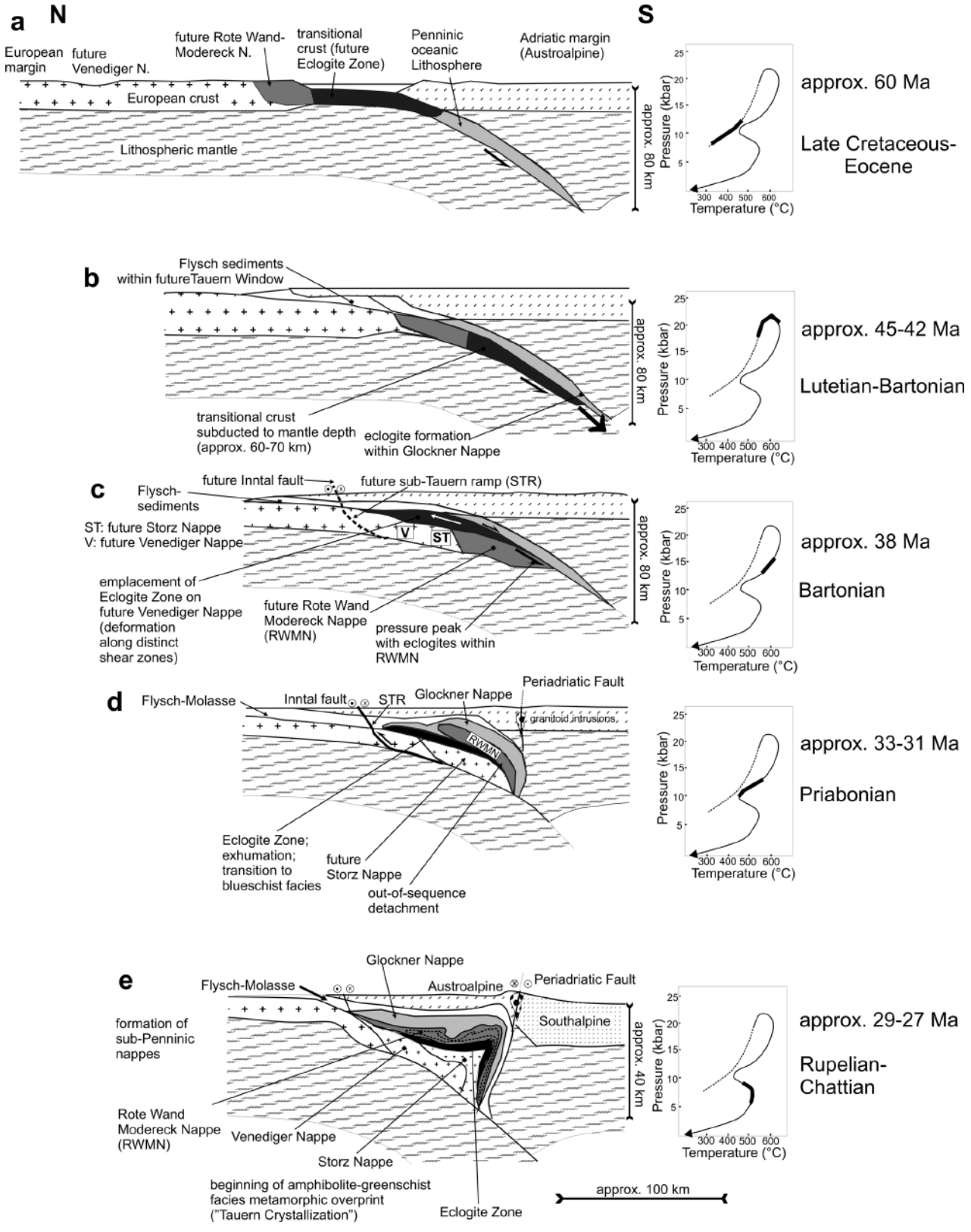

Fig. 9. Plate tectonic evolution of the Penninic units of the Eastern Alps during the Late Cretaceous and the Palaeogene (modified after Kurz et al., 2001b; Kurz & Froitzheim, 2002), including the P-T- evolution of the Eclogite Zone. V: Venediger Nappe; ST: Storz Nappe; STR: Sub-Tauern ramp; RWMN: Rote Wand – Modereck Nappe.

33–31 Ma, as indicated by the phengite ages from the eclogite mylonites. At this time, the Eclogite Zone and the Rote Wand – Modereck Nappe show nearly the same pressure conditions of approximately 10–11 kbar, despite the contrasting previous PT- evolution (Fig. 4). These contrasting PT- paths document a distinct tectonometamorphic evolution of the Eclogite Zone compared to the overlying units.

Timing of eclogite exhumation and nappe assembly coincides with the intrusion of granitoids along the Periadriatic fault south of the Tauern Window (Fig. 1), being explained by the breakoff of the Penninic oceanic slab (von Blanckenburg & Davies 1995). The contemporaneous exhumation of the Eclogite Zone and the adjacent units can therefore be interpreted to result from the rebound of the subducted buoyant continental crust of the European margin as a consequence of slab breakoff (Kurz 2005). Finally, this resulted in the detachment of the nappe stack from and the emplacement onto the European margin along the sub-Tauern ramp (Fig. 9c-e) (Ortner et al. 2006). In the upper crust displacement along the sub-Tauern ramp was partly transferred into the mainly sinistral Inntal fault (Fig. 9c-e) associated with the formation of fault-related intramontane molasse basins from Lower Oligocene times onwards (Rupelian, approximately 33 Ma) (Ortner & Sachsenhofer 1996). Therefore we conclude that the exhumation of the Eclogite Zone (33–31 Ma), granitoid intrusions along the Periadriatic fault, and the sedimentation of intramontane molasse deposits are closely related processes.

Subsequently, the Penninic and Subpenninic nappes were emplaced onto the European margin, probably by sinistral transpression along the sub-Tauern ramp, and contemporaneous with amphibolite to greenschist facies metamorphic overprint at approx. 28 Ma (Inger & Cliff 1994) (Fig. 9e).

9 Conclusions

1. Provided that detailed knowledge of the tectono-metamorphic history of the investigated rocks is available, $^{40}Ar/^{39}Ar$ dating of white mica can constrain early cooling subsequent to peak pressure conditions and eclogite deformation along the exhumation path.
2. White micas that formed under eclogite-facies metamorphic conditions retain their initial isotopic signature even when associated lithologies were affected by a later greenschist- to lower amphibolite-facies metamorphic overprint in case of heterogeneous advection and conduction of heat enabled the preservation of eclogite-facies assemblages.
3. If exhumation is accompanied by ductile shearing in distinct domains, then ductile deformation plays a more important role in the resetting of isotopic systems than temperature.
4. In the Eclogite Zone of the Tauern Window cooling of unfoliated eclogites occurred at the earliest around ca. 38 Ma ago; thus the pressure peak within the Eclogite Zone was reached prior to ca. 38 Ma.
5. Deformation under eclogite facies conditions proceeded along the exhumation path and eclogite mylonites cooled below 500–550 °C at ca. 32 Ma. From the pressure peak onwards, eclogitic condition prevailed for almost 8–10 Ma.
6. Emplacement of the Eclogite Zone and exhumation to blueschist facies metamorphic conditions occurred not before 32 Ma ago.
7. The pressure peak within the Rote Wand – Modereck Nappe (related to the burial of this unit) was reached close to 39 Ma.
8. Geochronological ages on exhumation-related syn-deformational eclogite cooling (33–31 Ma) are supported by the ages of granitoid intrusion along the Periadriatic Fault and the sedimentation of intramontane molasses deposits, all being related to the rebound of the subducted buoyant continental crust of the European margin subsequent to slab breakoff.

Acknowledgements

Parts of the study were supported by a grant of the Austrian Research Foundation (grant P9918-GEO; J1986-GEO, J2155). We gratefully acknowledge the formal reviews by Bernhard Fügenschuh and Ralf Schuster and their constructive comments.

REFERENCES

Behrmann, J.H., Ratschbacher, L. 1989. Archimedes revisited: a structural test of eclogite emplacement models in the Austrian Alps. Terra Nova 1, 242–252.

Bossé, V., Féraud, G., Ballévre, G., Peucat, J.-J. & Corsini, M. 2005. Rb-Sr and $^{40}Ar/^{39}Ar$ ages in blueschists from the Ile de Groix (Armorican Massif, France): Implications for closure mechanisms in isotopic systems. Chemical Geology 220, 21–45.

Chopin, C. & Maluski, H. 1980. ^{40}Ar-^{39}Ar Dating of High Pressure Metamorphic Micas From the Gran Paradiso Area (Western Alps): Evidence Against the Blocking Temperature Concept. Contributions to Mineralogy and Petrology 74, 109–122.

Cliff, R.A., Droop, G.T.R. & Rex, D.C. 1985. Alpine metamorphism in the south-east Tauern Window, Austria: II. heating, cooling and uplift rates. Journal of metamorphic Geology 3, 403–415.

Dachs, E. 1986. High-pressure mineral assemblages and their breakdown products in metasediments south of the Grossvenediger, Tauern Window, Austria. Schweizerische Mineralogische und Petrographische Mitteilungen 66, 145–161.

Dachs, E. 1990. Geothermobarometry in metasediments of the southern Grossvenediger area (Tauern Window, Austria). Journal of metamorphic Geology 8, 217–230.

Dachs, E. & Proyer, A. 2001. Relics of high-pressure metamorphism from the Grossglockner region, Hohe Tauern, Austria: Pragenetic evolution and PT-paths of retrogressed eclogites. European Journal of Mineralogy 13, 67–86.

Dachs, E. & Proyer, A. 2002. Constraints on the duration of high-pressure metamorphism in the Tauern Window from diffusion modelling of discontinous growth zones in eclogite garnet. Journal of metamorphic Geology 20, 769–780.

Droop, G.T. R. 1985. Alpine metamorphism in the south-east Tauern Window, Austria, I. P-T variations in space and time. Journal of metamorphic Geology 3, 371–402.

Droop, G.T.R., Lombardo, B. & Pognate, U. 1990. Formation and distribution of eclogite facies rocks in the Alps. In: Carswell, D.A. (Ed.). Eclogite Facies Rocks. Blackie/Glasgow, 225–259.

Dunlap, W.J. 1997. Neocrystallization or cooling? $^{40}Ar/^{39}Ar$ ages of white micas from low-grade mylonites. Chemical Geology 143, 181–203.

Ernst, W.G. 2006. Preservation/exhumation of ultrahigh-pressure subduction complexes. Lithos 92, 321–335.

Frank, W., Höck, V. & Miller, C. 1987. Metamorphic and tectonic history of the central Tauern Window. In: Flügel, H.W. & Faupl, P. (Eds.): Geodynamics of the Eastern Alps. Deuticke/Vienna, 34–54.

Frisch, W. 1979. Tectonic progradation and plate tectonic evolution of the Alps. Tectonophysics 60, 121–139.

Frisch, W. 1980. Plate motions in the Alpine region and their correlation to the opening of the Atlantic Ocean. Mitteilungen der Österreichischen Geologischen Gesellschaft 71/72, 45–48.

Gleissner, P., Glodny, J. & Franz, G. 2007. Rb-Sr isotopic dating of pseudomorphs after lawsonite in metabasalts from the Glockner nappe, Tauern Window, Eastern Alps. European Journal of Mineralogy 19, 723–734.

Glodny, J., Ring, U., Kühn, A., Gleissner, P. & Franz, G. 2005. Crystallization and very rapid exhumation of the youngest Alpine eclogites (Tauern Window, Eastern Alps) from Rb/Sr mineral assemblage analysis. Contributions to Mineralogy and Petrology 149, 699–712.

Glodny, J., Ring, U. & Kühn, A. 2008. Coeval high-pressure metamorphism, thrusting, strike-slip and extensional shearing in the Tauern Window, Eastern Alps. Tectonics 27, TC4004, doi: 10.1029/2007TC002193.

Hames, W.E. & Bowring, S.A. 1994. An empirical evaluation of the argon diffusion geometry in muscovite. – Earth and Planetary Scientific Letters 124, 161–167.

Hames, W.E. & Cheney, J.T. 1997. On the loss of ^{40}Ar from muscovite during polymetamorphism. Geochimica and Cosmochimica Acta 61, 3863–3872.

Hammerschmidt, K. & Frank, E. 1991. Relics of high-pressure metamorphism in the Lepontine Alps (Switzerland) – $^{40}Ar/^{39}Ar$ and microprobe analyses on white micas. Schweizerische Mineralogische und Petrographische Mitteilungen 71, 261–274.

Handler, R., Dallmeyer, R.D., Neubauer, F. & Frank, W. 1993. Deformation and isotopic resetting in low-grade metamorphic rocks. Abstracts supplement No. 2 to Terra Nova 5, p. 13.

Handler, R., Neubauer, F., Velichkova, S.H. & Ivanov, Z. 2004: $^{40}Ar/^{39}Ar$ age constraints on the timing of magmatism and post-magmatic cooling in the Panagyurishte region, Bulgaria. – Schweizerische Mineralalogischen und Petrographische Mitteilungen, 84 (1–2), 119–132.

Heizler, M.T. & Harrison, T.M. 1988. Multiple trapped argon isotopic components revealed by $^{40}Ar/^{39}Ar$ isochron analysis. Geochimica et Cosmochimica Acta 52, 1295–1303.

Holland, T.J.B. 1979. High water activities in the generation of high pressure kyanite eclogites in the Tauern Window, Austria. Journal of Geology 87, 1–27.

Hoschek, G. 2001. Thermobarometry of metasediments and metabasites from the Eclogite zone of the Hohe Tauern, Eastern Alps, Austria. Lithos 59, 127–150.

Inger, S. & Cliff, R.A. 1994. Timing of metamorphism in the Tauern Window, Eastern Alps: Rb-Sr ages and fabric formation. Journal of Metamorphic Geology 12, 695–707.

Kelley, S. 1995. Ar-Ar dating by laser microprobe. In: Potts, P.J., Bowles, J.F.W., Reed, S.J. B. & Cave. M. R. (Eds.): Microprobe Techniques in the Earth Sciences. The mineralogical Society Series 6, 327–358.

Kirschner, D.L., Cosca, M.A., Masson, H. & Hunziker, J.C. 1996. Staircase $^{40}Ar/^{39}Ar$ spectra of fine-grained white mica: Timing and duration of deformation and empirical constraints on argon diffusion. Geology 24, 747–751.

Kretz, R. 1983. Symbols for rock-forming minerals. American Mineralogist 68, 277–279.

Kurz, W. 2005. Constriction during exhumation: Evidence from eclogite microstructures. Geology 33, 37–40.

Kurz, W. & Froitzheim, N. 2002. The exhumation of eclogite-facies metamorphic rocks – a review of models confronted with examples from the Alps. International Geology Review 44, 702–743.

Kurz, W., Neubauer, F. & Genser, J. 1996. Kinematics of Penninic nappes (Glockner Nappe and basement-cover nappes) in the Tauern Window (Eastern Alps, Austria) during subduction and Penninic-Austroalpine collision. Eclogae Geologicae Helvetiae 89, 573–605.

Kurz, W., Neubauer, F. & Dachs, E. 1998a. Eclogite meso- and microfabrics: implications for the burial and exhumation history of eclogites in the Tauern Window (Eastern Alps) from P-T-d paths. Tectonophysics 285, 183–209.

Kurz, W., Neubauer, F., Genser, J. & Dachs, E. 1998b. Alpine geodynamic evolution of passive and active continental margin sequences in the Tauern Window (eastern Alps, Austria, Italy): a review. International Journal of Earth Sciences (Geologische Rundschau) 87, 225–242.

Kurz, W., Fritz, H., Piller, W.E., Neubauer, F. & Genser, J. 2001a. Overview of the Palaeogene of the Eastern Alps. In: Piller, W.E. & Rasser, M. (Eds.), Palaeogene of the Eastern Alps: Österreichische Akademisch wissenschaftliche, Schriftenreihe der erdwissenschaftlichen Kommission 14, 11–56.

Kurz, W., Neubauer, F., Genser, J., Unzog, W. & Dachs, E. 2001b. Tectonic Evolution of Penninic Units in the Tauern Window during the Palaeogene: Constraints from Structural and Metamorphic Geology. In: Piller, W.E. & Rasser, M. (Eds.): Paleogene of the Eastern Alps: Österreichische Akademisch wissenschaftliche, Schriftenreihe der erdwissenschaftlichen Kommission 14, 11–56.

Kurz, W., Jansen, E., Hundenborn, R., Pleuger; J., Schäfer, W. & Unzog, W. 2004. Microstructures and Crystallographic Preferred Orientations of omphacite in Alpine eclogites: implications for the exhumation of (ultra-)high-pressure units. Journal of Geodynamics 37, 1–55.

Lips, A.L.W., White, S.H. & Wijbrans, J.R. 1998. $^{40}Ar/^{39}Ar$ laserprobe direct dating of discrete deformational events: a continuous record of early Alpine tectonics in the Pelagonian Zone, NE Aegean area, Greece. Tectonophysics 298, 133–153.

Lister, G.S. & Baldwin, S.L. 1996. Modelling the effect of arbitrary P-T-t histories on argon diffusion in minerals using the MacArgon program for the Apple Macintosh. Tectonophysics 253, 83–109.

Miller, C. 1974. On the metamorphism of the eclogites and high-grade blueschists from the Penninic Terrane of the Tauern Window, Austria. Schweizerische Mineralogische und Petrographische Mitteilungen 54, 371–384.

Müller, W., Dallmeyer, R.D., Neubauer, F. & Thöni, M. 1999. Deformation-induced resetting of Rb/Sr and 40Ar/39Ar mineral systems in a low-grade, polymetamorphic terrane (Eastern Alps, Austria). Journal of the geological Society of London 156, 261–278.

Neubauer, F., Genser, J. & Handler, R. 2000. The Eastern Alps: Result of a two-stage collision process. Mitteilungen der Österreichischen Geologischen Gesellschaft 92, 117–134.

Ortner, H. & Sachsenhofer, R. 1996: Evolution of the Lower Inntal Tertiary and Constraints on the Development of the Source Area. In: Liebl, W. & Wessely, G. (Eds): Oil and Gas in Alpidic Thrust Belts and Basins of Central and Eastern Europe. EAEG Special Publication 5, 237–247.

Ortner, H., Reiter, F. & Brandner, R. 2006. Kinematics of the Inntal shear zone-sub- Tauern ramp fault system and the interpretation of the TRANSALP seismic section, Eastern Alps, Austria. Tectonophysics 414, 241–258.

Proyer, A. 2003. Metamorphism of pelites in NKFMASH – a new petrogenetic grid with implications for the preservation of high-pressure mineral assemblages during exhumation. Journal of metamorphic Geology 21, 493–509.

Proyer, A., Dachs, E. & Kurz, W. 1999. Relics of high-pressure metamorphism in the Glockner region, Hohe Tauern, Austria: Textures and mineral chemistry of retrogressed eclogites. Mitteilungen der Österreichischen Geologischen Gesellschaft 90, 43–55.

Raith, M., Mehrens, C. & Thöle, W. 1980. Gliederung, tektonischer Bau und metamorphe Entwicklung der penninischen Serien im südlichen Venediger-Gebiet, Osttirol. Jahrbuch der Geologischen Bundesanstalt 123, 1–37.

Ratschbacher, L., Dingeldey, C., Miller, C., Hacker, B.R. & McWilliams, M.O. 2004. Formation, subduction, and exhumation of Penninic oceanic crust in the Eastern Alps: time constraints from $^{40}Ar/^{39}Ar$ geochronology. Tectonophysics 394, 155–170.

Reddy, S.M., Cliff, R.A. & East, R. 1993. Thermal history of the Sonnblick Dome, south-east Tauern Window, Austria: Implications for Heterogenous uplift within the Pennine basement. International Journal of Earth Sciences (Geologische Rundschau) 82, 667–675.

Scaillet, S. 1998. K-Ar ($^{40}Ar/^{39}Ar$) Geochronology of Ultrahigh Pressure Rocks. In: Hacker, B.R. & Liou, J. G: (eds.): When Continents Collide: Geodynamics of Ultrahigh Pressure Rocks. Kluwer Academic Publishers/Dordrecht – Boston – London, 161–201.

Schmid, S.M., Fügenschuh, B., Kissling, E. & Schuster, R. 2004. Tectonic map and overall architecture of the Alpine orogen. Eclogae geologicae Helvetiae 97, 93–117.

Schuster, R. & Kurz, W. 2005. Eclogites in the Eastern Alps: High-pressure metamorphism in the context of Alpine orogeny. Mitteilungen der Österreichischen Mineralogischen Gesellschaft 150, 183–198.

Selverstone, J. 1993. Micro- to macroscale interactions between deformational and metamorphic processes, Tauern Window, Eastern Alps. Schweizerische Mineralogische und Petrographische Mitteilungen 73, 229–239.

Selverstone, J., Spear, F.S., Franz, G. & Morteani, G. 1984. High- Pressure Metamorphism in the SW Tauern Window, Austria: P-T Paths from Hornblende- Kyanite- Staurolite Schists. Journal of Petrology 25, 501–531.

Spear, F.S. & Franz, G. 1986. P-T evolution of metasediments from the Eclogite Zone, south central Tauern Window, Austria. Lithos 25, 219–234.

Stöckhert, B., Massonne, H-J. & Nowlan, E.U. 1997. Low differential stress during high-pressure metamorphism: The microstructural record of a metapelite from the Eclogite Zone, Tauern Window, Eastern Alps. Lithos 41, 103–118.

Stuart, F.M. 2002. The exhumation history of orogenic belts from $^{40}Ar/^{39}Ar$ ages of detrital micas. Mineralogical Magazine 66, 121–135.

Thöni, M. 2006. Dating eclogite-facies metamorphism in the Eastern Alps – approaches, results, interpretations: a review. Mineralogy and Petrology 88, 123–148.

TRANSALP Working Group 2002. First deep seismic reflection images of the Eastern Alps reveal giant crustal wedges and transcrustal ramps. Geophysical Research Letters 29, 92–2–92–4.

TRANSALP working group 2006. TRANSALP – A transect through a young collisional orogen: Introduction. Tectonophysics 414, 1–7.

Villa, I.M. 1998. Isotopic closure. Terra Nova 10, 42–47.

von Blanckenburg, F. & Davies, H.J. 1995. Slab breakoff: A model for syncollisional magmatism and tectonics in the Alps. Tectonics 14, 120–131.

von Blanckenburg, F.& Villa, I.M. 1988. Argon retentivity and argon excess in amphiboles from the garbenschists of the Western Tauern Window, Eastern Alps. Contributions to Mineralogy and Petrology 100, 1–11.

von Blanckenburg, F., Villa, I.M., Baur, H., Morteani, G. & Steiger, R.H. 1989. Time Calibration of a PT-path from the Western Tauern Window, Eastern Alps: the problem of closure temperatures. Contributions to Mineralogy and Petrology 101, 1–11.

Zimmermann, R., Hammerschmidt, K. & Franz, G. 1994. Eocene high pressure metamorphism in the Penninic units of the Tauern Window (Eastern Alps):evidence from ^{40}Ar-^{39}Ar dating and petrological investigations. Contributions to Mineralogy and Petrology 117, 175–186.

Manuscript received 11 October, 2007
Revision accepted 5 February, 2008
Published Online first October 22, 2008
Editorial Handling: Stefan Schmid, Stefan Bucher

Electronic supplementary material: The online version of this article (DOI: 10.1007/s00015-1281-1) contains supplementary material, which is available to authorized authors.

Appendix I. Location of samples used for microprobe analyses and $^{40}Ar/^{39}Ar$ dating.

For samples 1–4 PT-data have been published by KURZ et al. (1998a). To allow easy correlation of the samples, the sample numbers used by KURZ et al. (1998a) are given in parentheses. Numbers and names of the Austrian topographic map ÖK50 are given.

Sample 1 (WK526): Eclogite-mylonite of the Eclogite Zone; Dorfertal 750 m SE of the hut "Johanneshütte"; ÖK50, sheet 152 Matrei; 12° 20' 21" E, 47° 03' 34" N.

Sample 2 (WK538): Eclogite-mylonite of the Eclogite Zone; Timmeltal: north-west-shore of lake "Eissee"; ÖK50, sheet 152 Matrei; 12° 23' 10" E, 47° 03' 56" N.

Sample 3 (WK540): Eclogite-mylonite of the Eclogite Zone; Timmeltal: west-shore of lake "Eissee"; ÖK50, sheet 152 Matrei; 12° 23' 01" E, 47° 03' 48" N.

Sample 4 (WK557): Fine-grained eclogite of the Eclogite Zone; Frosnitztal, 250 m north of location "Steinsteig"; ÖK50, sheet 152 Matrei; 12° 27' 01" E, 47° 04' 31" N.

Sample 5: Calcite marble of the Rote Wand – Modereck nappe; location "Hochtor" at the road "Glocknerstraße"; ÖK50, sheet 154 Rauris; 12° 50' 34" E, 47° 05' 04" N.